Available online at www.sciencedirect.com

SciVerse ScienceDirect

Ceramics International 38 (2012) 5045–5051

CERAMICS INTERNATIONAL

www.elsevier.com/locate/ceramint

Concentration effects on the upconversion luminescence in Ho^{3+}/Yb^{3+} co-doped $NaGdTiO_4$ phosphor

Yunfeng Jiang [a], Rensheng Shen [a], Xiangping Li [a,b,*], Jinsu Zhang [b], Hua Zhong [b], Yue Tian [b], Jiashi Sun [b], Lihong Cheng [b], Haiyang Zhong [b], Baojiu Chen [b,**]

[a] School of Physics and Optoelectronic Engineering, Dalian University of Technology, Dalian, Liaoning, 116024, PR China
[b] Department of Physics, Dalian Maritime University, Dalian, Liaoning 116026, PR China

Received 24 February 2012; received in revised form 1 March 2012; accepted 1 March 2012
Available online 10 March 2012

Abstract

Ho^{3+}/Yb^{3+} co-doped $NaGdTiO_4$ phosphors were synthesized by a solid-state reaction method. The upconversion (UC) luminescence characteristics excited by 980 nm laser diode were systematically investigated. Bright green UC emission centered at 551 nm accompanied with weak red and near infrared (NIR) UC emissions centered at 652 and 761 nm were observed. The dependence of UC emission intensity on excitation power density showed that all of green, red and NIR UC emissions are involved in two-photon process. The UC emission mechanisms were discussed in detail. Concentration dependence studies indicated that Ho^{3+} and Yb^{3+} concentrations had significant influences on UC luminescence intensity and the intensity ratio of the red UC emission to that of the green one. Rate equations were established based on the possible UC mechanisms and a theoretical formula was proposed to describe the concentration dependent UC emission. The UC luminescence properties of the presented material was evaluated by comparing with commercial $NaYF_4:Er^{3+}$, Yb^{3+} phosphor, and our sample showed a high luminescence efficiency and good color performance, implying potential applications in a variety of fields.

Keywords: Solid-state reaction; Upconversion luminescence; $NaGdTiO_4$; Concentration dependence

1. Introduction

Recently, photon upconversion (UC), via which the long-wavelength lights can be converted into short-wavelength lights, has been paid much attention due to its promising applications in three-dimensional displays, optical data storage, medical diagnostics, sensors, and optical amplifiers, etc. [1–5]. Lanthanide ions are often employed as UC luminescence centers due to the intra-4f transitions which are barely affected by external crystal field since the electrons at 4f orbit are shielded by the filled outer 5s and 5p orbits. Among the various lanthanide ions studied for UC luminescence, Ho^{3+} has been attracted considerable attention owing to its dominant green UC emission [6]. However, there is no such an f–f transition from ground state of Ho^{3+} whose energy matches the energy of one 980 nm photon, so the ground state absorption (GSA) of Ho^{3+} is unlikely to occur, therefore, sensitizing ion is needed to obtain high UC efficiency from Ho^{3+}. Yb^{3+} is commonly used as sensitizer in UC luminescence to harvest pump photons and subsequently promotes neighboring activator ions to excited states because of its some peculiar characteristics: (1) simple two-level structure of Yb^{3+} ensures high quenching concentration; (2) large absorption cross-section of Yb^{3+} at 980 nm leads to efficient absorption of pump energy; (3) large spectral overlap between Yb^{3+} emission ($^2F_{5/2} \rightarrow {}^2F_{7/2}$) and Ho^{3+} absorption ($^5I_8 \rightarrow {}^5I_6$) drives energy transfer (ET) from Yb^{3+} to Ho^{3+} efficient; and (4) alike chemical properties and similar ionic radius between Yb^{3+} and Ho^{3+} make their homogenous doping easier [7,8]. Thus, UC luminescence of Ho^{3+} in Ho^{3+}/Yb^{3+} co-doped systems has been extensively studied, and predominant green UC emissions have been obtained especially in low phonon energy hosts, such as fluoride and sulfide matrix [9–17]. However, due to the high cost, poor

* Corresponding author at: Department of Physics, Dalian Maritime University, Dalian, Liaoning 116026, PR China. Tel.: +86 41184728909; fax: +86 41184728909.
** Corresponding author. Tel.: +86 41184728909; fax: +86 41184728909.
E-mail addresses: lixp@dlmu.edu.cn (X. Li), Chembj@sohu.com (B. Chen).

0272-8842/$36.00
doi:10.1016/j.ceramint.2012.03.006

chemical durability and thermal stability, rare-earth ions (RE^{3+}) doped fluoride and sulfide based materials cannot meet the practical applications well, though they possess high UC efficiencies. Therefore, exploring novel UC materials is essential. Oxide materials as one of the feasible UC luminescence hosts have been extensively studied due to their higher melting point, better chemical stability and easier preparation than those of fluoride materials [18–22]. Among the oxide compounds, RE^{3+} (such as Gd^{3+}, Y^{3+} and Lu^{3+}) contained inorganic compounds with low phonon energies are preferable hosts for UC luminescence.

In this work, titanate was chosen as the host due to its special properties, such as low cost, easy preparation, excellent thermal and chemical stabilities. $NaGdTiO_4$:Ho^{3+}/Yb^{3+} UC phosphors were synthesized by a conventional solid-state reaction method. The concentration and power dependences of UC luminescence and UC mechanism were systematically studied. The UC luminescence properties of the presented material were estimated and the result indicated that our sample had high luminescence efficiency and good color performance.

2. Experimental

2.1. Chemicals

Yb_2O_3 (99.99%), Ho_2O_3 (99.99%), TiO_2 (99.0%, body type) and Na_2CO_3 (99.8%, anhydrous) were used as starting materials. Meanwhile, excessive Na_2CO_3 was employed to improve the chemical reaction.

2.2. Sample preparation

Two sets of Ho^{3+}/Yb^{3+} co-doped $NaGdTiO_4$ samples were synthesized via a conventional solid-state reaction method. In the first set, Ho^{3+} concentration is fixed to be 0.5 mol%, and Yb^{3+} concentrations are 1, 3, 5, 7, 10, 15 and 20 mol%. In the second set, Yb^{3+} concentration is fixed to be 5 mol%, and Ho^{3+} concentrations are 0.05, 0.1, 0.3, 0.5, 1, 3 and 5 mol%. The concentrations of Ho^{3+} and Yb^{3+} mentioned in this paper are molar percentages if without specific statement. Firstly, the starting materials were weighed according to certain stoichiometric ratio. Secondly, each weighed bitch was blended in an agate mortar and thoroughly ground. Then the obtained uniform mixture was put into alumina crucible and calcined in a muffle furnace at 1000 °C for 4 h. Finally, the corresponding phosphors were obtained when the furnace cooled naturally down to room temperature.

2.3. Sample characterization

The crystal phase identification was performed via X-ray diffraction (XRD) by using a Japan Shimadzu XRD-6000 diffractometer with Cu Kα radiation (λ = 0.15406 nm) source. The XRD data in the 2θ range from 5° to 60° were collected in a scanning mode with a step size of 0.02° and a scanning rate of 2.0° min^{-1}. The UC emission spectra were obtained by a Hitachi F-4600 fluorescence spectrometer upon 980 nm LD excitation with a maximum power of 2 W. All of the measurements were performed at room temperature.

3. Results and discussion

3.1. Structural characterization

The XRD patterns for the samples doped with various Yb^{3+} and Ho^{3+} concentrations were measured. Fig. 1 shows the XRD patterns of the samples with fixed Ho^{3+} concentration of 0.5% and various Yb^{3+} concentrations of 1, 10 and 20%, as a representative. As can be seen, all three samples exhibit similar profile, and the positions of most of the diffraction peaks are in good agreement with the standard pattern of orthorhombic $NaGdTiO_4$ reported in JCPDS 86-0830 as shown in Fig. 1(a). However, a diffraction peak located at 28.70° marked by open square was also detected, which can be assigned to the overlapped diffraction peaks belonging to $NaGdTiO_4$ and Gd_2O_3 (JCPDS No. 86-2477), indicating that there is some unspent Gd_2O_3. Therefore, the reaction conditions such as the temperature and the amount of flux could be further optimized to obtain pure $NaGdTiO_4$ phosphors.

3.2. UC luminescence spectroscopy and mechanism analysis

Fig. 2 shows the UC emission spectra for the samples doped with 0.5% Ho^{3+}/1% Yb^{3+} and 0.5% Ho^{3+}/20% Yb^{3+} excited by 980 nm LD working at different currents. In the spectra, dominant green emissions centered at around 551 nm corresponding to ($^5S_2$, $^5F_4$) → $^5I_8$ transitions of Ho^{3+} are observed, accompanying with red and near infrared (NIR) emission bands located at around 669 and 761 nm corresponding to $^5F_5$ → $^5I_8$ and ($^5S_2$, $^5F_4$) → $^5I_7$ transitions. The red and the NIR UC emissions are much weaker than the green one at low Yb^{3+} concentration, but the red UC emission is strong in the

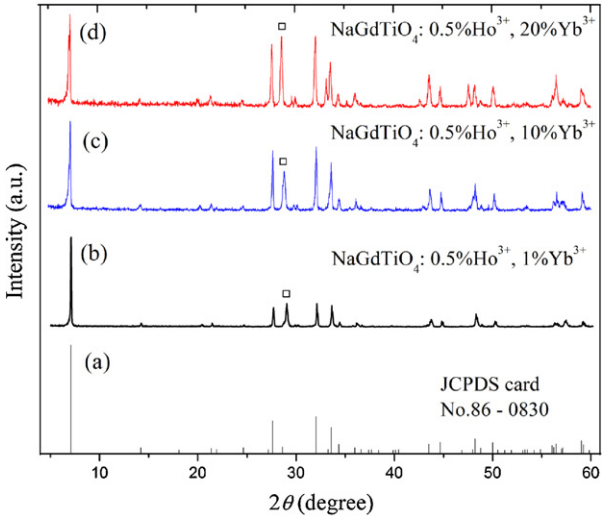

Fig. 1. XRD patterns for the orthorhombic $NaGdTiO_4$ (JCPDS Card No. 86-0830) (a), the $NaGdTiO_4$ samples doped with 0.5% Ho^{3+}/1% Yb^{3+} (b), 0.5% Ho^{3+}/10% Yb^{3+} (c) and 0.5% Ho^{3+}/20% Yb^{3+} (d).

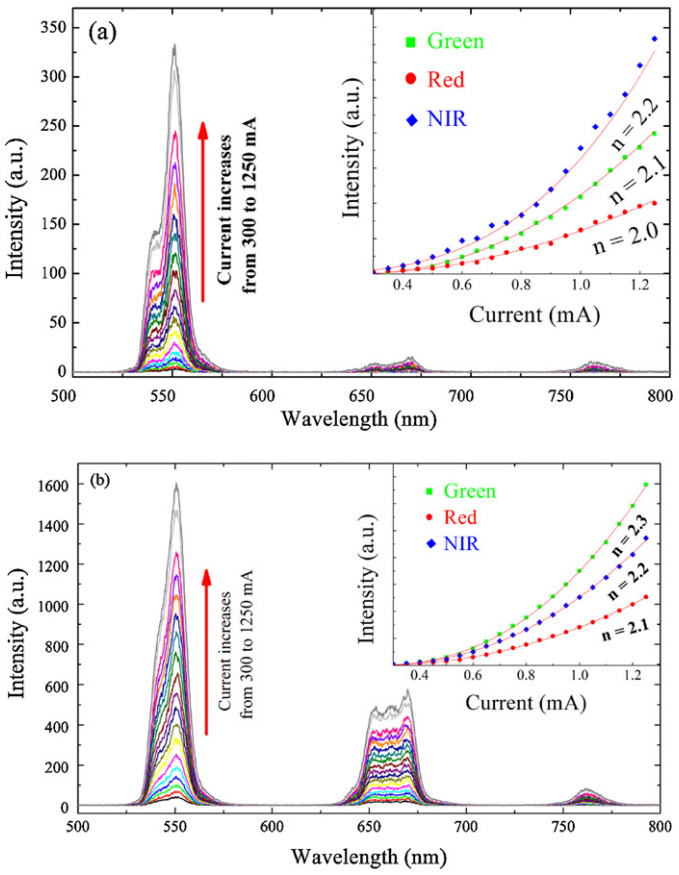

Fig. 2. UC emission spectra excited by 980 nm LD working at different currents for the samples doped with 0.5% Ho^{3+}/1% Yb^{3+} (a) and 0.5% Ho^{3+}/20% Yb^{3+} (b).

sample with high Yb^{3+} concentration. From Fig. 2, it can also be seen that with the increase of LD working current, all of the UC emission intensities for different transitions increase. The insets of Fig. 2 illustrate the dependences of green, red and NIR UC integrated emission intensities on LD working current for both the samples doped with 0.5% Ho^{3+}/1% Yb^{3+} and 0.5% Ho^{3+}/20% Yb^{3+}.

It is well known that the output power of LD depends linearly on its working current, and can be expressed as [23]:

$$P = P_0(i - i_0) \quad (1)$$

where i_0 is the threshold current of LD, P_0 is a constant. For an n-photon process, the UC emission intensity is proportional to P^n. Therefore, the relationship between UC emission intensity I_{up} and LD working current can be described as:

$$I_{up} = I_0(i - i_0)^n \quad (2)$$

By fitting the experimental data in the insets of Fig. 2 with Eq. (2), the n values are obtained to be 2.1, 2.3 for green emissions, 2.0, 2.1 for red emissions and 2.2, 2.2 for NIR emissions for the samples doped with 0.5% Ho^{3+}/1% Yb^{3+} and 0.5% Ho^{3+}/20% Yb^{3+}, respectively. All these values of n are close to 2, indicating that all of green, red and NIR UC emissions are involved in two-photon process.

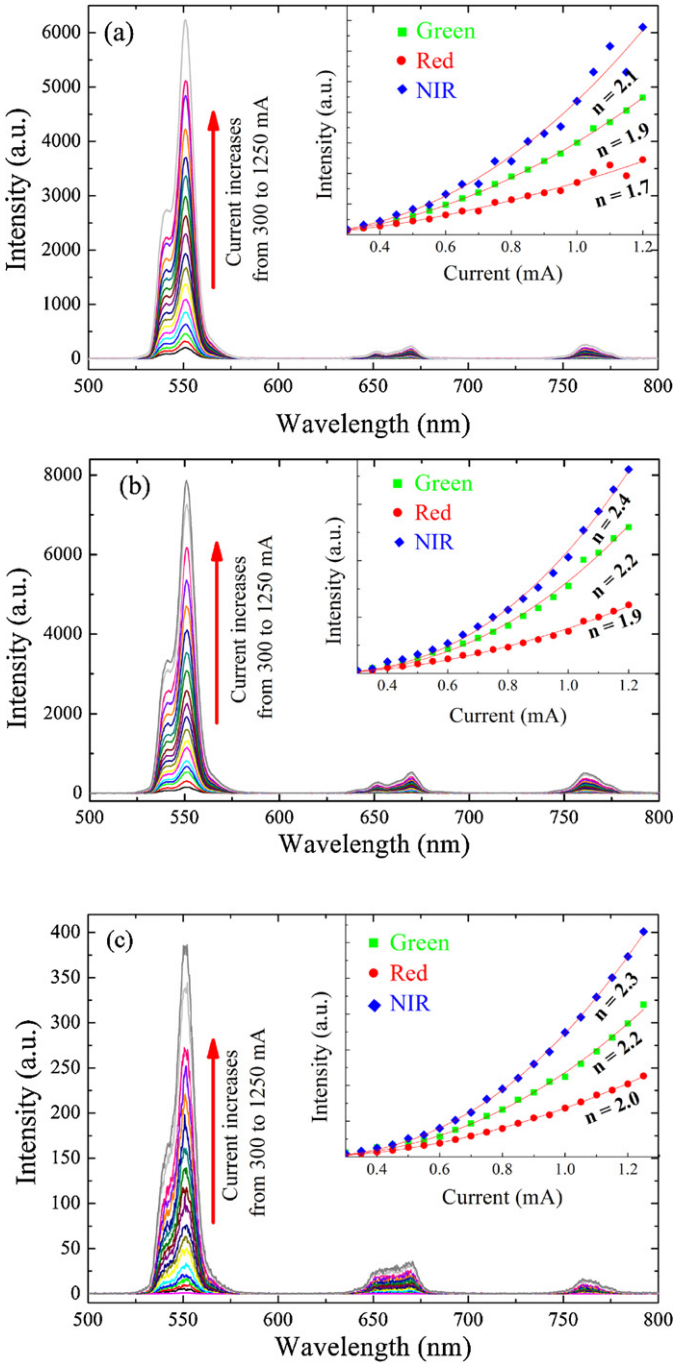

Fig. 3. UC emission spectra excited by 980 nm LD working at different currents for the samples doped with 0.05% Ho^{3+}/5% Yb^{3+} (a), 0.1% Ho^{3+}/5% Yb^{3+}(b) and 3% Ho^{3+}/5% Yb^{3+} (c).

Fig. 3 displays the UC emission spectra for the samples doped with fixed Yb^{3+} concentration of 5% and various Ho^{3+} concentrations of 0.05, 0.1 and 3% upon excitation of 980 nm LD working at different currents. As can be seen, all of the spectra have the same profile and the intensity of each UC emission increases with the increase of working current, indicating that the working current of LD has no influences on the branching ratio of Ho^{3+} UC luminescence. The dependences of integrated UC emission intensities on LD working current are shown in the insets of Fig. 3. In an analogous way as

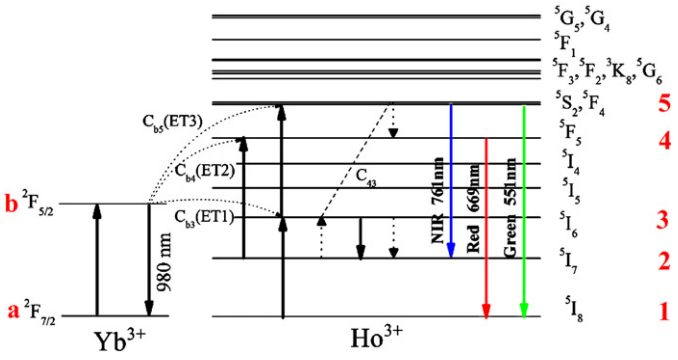

Fig. 4. Energy level diagrams of Ho^{3+} and Yb^{3+} and the possible populated ways for ($^5S_2$, $^5F_4$) and $^5F_5$ levels of Ho^{3+}. Solid and dashed lines represent absorptive/radiative transitions and ET/nonradiative relaxation, respectively.

above, the numerical fittings are also carried out and the values of *n* are confirmed to be 1.9, 2.2, 2.2 for green emissions, 1.7, 1.9, 2.0 for red emissions and 2.1, 2.4, 2.3 for NIR emissions for the samples doped with 0.05, 0.1 and 3% Ho^{3+}, respectively. The *n* values for all of the transitions mentioned above are close to 2, indicating that all UC emissions are also involved in two-photon process.

From above results, it can be concluded that the two-photon process is dominant in Ho^{3+}/Yb^{3+} co-doped $NaGdTiO_4$ phosphors and independent from Ho^{3+} and Yb^{3+} concentrations in our experimental concentration range. Actually, the mechanism of two-photon UC in Ho^{3+}/Yb^{3+} co-doped system has been well known [24]. Fig. 4 shows the typical energy levels diagram and UC luminescence processes in Ho^{3+}/Yb^{3+} co-doped system excited by 980 nm LD. When an Yb^{3+} ion is excited to $^2F_{5/2}$ level by a 980 nm photon, its energy can be transferred to a neighboring Ho^{3+}. Ho^{3+} is excited to $^5I_6$ level by ET process. Through another ET process, $^2F_{5/2}(Yb^{3+}) + {}^5I_6(Ho^{3+}) \rightarrow {}^2F_{7/2}(Yb^{3+}) + (^5S_2, {}^5F_4)(Ho^{3+})$, ($^5S_2$, $^5F_4$) levels of Ho^{3+} are populated. Then green and NIR emissions are obtained through radiative transitions from ($^5S_2$, $^5F_4$) to $^5I_8$ and $^5I_7$ levels. For the red emission come from $^5F_5 \rightarrow {}^5I_8$ transition, there are usually two possible ways populating $^5F_5$ level. First, it could be populated by nonradiative relaxation from the upper ($^5S_2$, $^5F_4$) levels. Second, after the population of $^5I_6$ level (Ho^{3+}) by ET process, Ho^{3+} in the metastable $^5I_6$ level relaxed into $^5I_7$ level first, followed with another ET process, $F_{5/2}(Yb^{3+}) + {}^5I_7(Ho^{3+}) \rightarrow {}^2F_{7/2}(Yb^{3+}) + {}^5F_5(Ho^{3+})$.

3.3. Concentration dependences of UC emission

The UC emission spectra for all prepared samples were measured under the same experimental conditions. In these measurements, the power density of LD is estimated to be about 15 W/cm^2 (corresponding working current is 1000 mA). The integrated intensities for green, red and NIR UC emissions were calculated and Fig. 5 displays the dependences of the integrated emission intensities on Ho^{3+} and Yb^{3+} concentrations for the two-set samples. It can be seen from Fig. 5(a) that as Yb^{3+} concentration increases, the green and the NIR UC emission intensities increase first and then decrease, but the red UC emission intensity increases continuously. When Yb^{3+} concentration is 5%, the intensities of the green and the NIR UC emissions reach the maximum values. For higher Yb^{3+} concentration, the green and the NIR UC emission intensities decrease, which may be mainly caused by the energy back transfer (EBT) from Ho^{3+} to Yb^{3+} ($^5S_2$, $^5F_4$) (Ho) + $^2F_{7/2}$(Yb) → $^5I_6$(Ho) + $^2F_{5/2}$(Yb) [25]. The higher Yb^{3+} concentration, the higher ratio between EBT from Ho^{3+} to Yb^{3+} and ET from Yb^{3+} to Ho^{3+}. For the red UC emission, the intensity kept increase in the studied Yb^{3+} concentration range (1–20%), indicating that the population of Ho^{3+} $^5F_5$ level is far higher than its depopulation. The opposed variation trend for the red and the green UC emission intensities demonstrates that the population of Ho^{3+} $^5F_5$ level is not only realized by nonradiative relaxation from ($^5S_2$, $^5F_4$) levels [26], but also the well-known ET process $^2F_{5/2}$(Yb) + $^5I_7$(Ho) → $^2F_{7/2}$(Yb) + $^5F_5$(Ho) [27]. Besides, the cross-relaxation process ($^5S_2$, $^5F_4$)(Ho) + $^5I_7$(Ho) → $^5I_6$(Ho) + $^5F_5$(Ho) may also be a possible way to realize

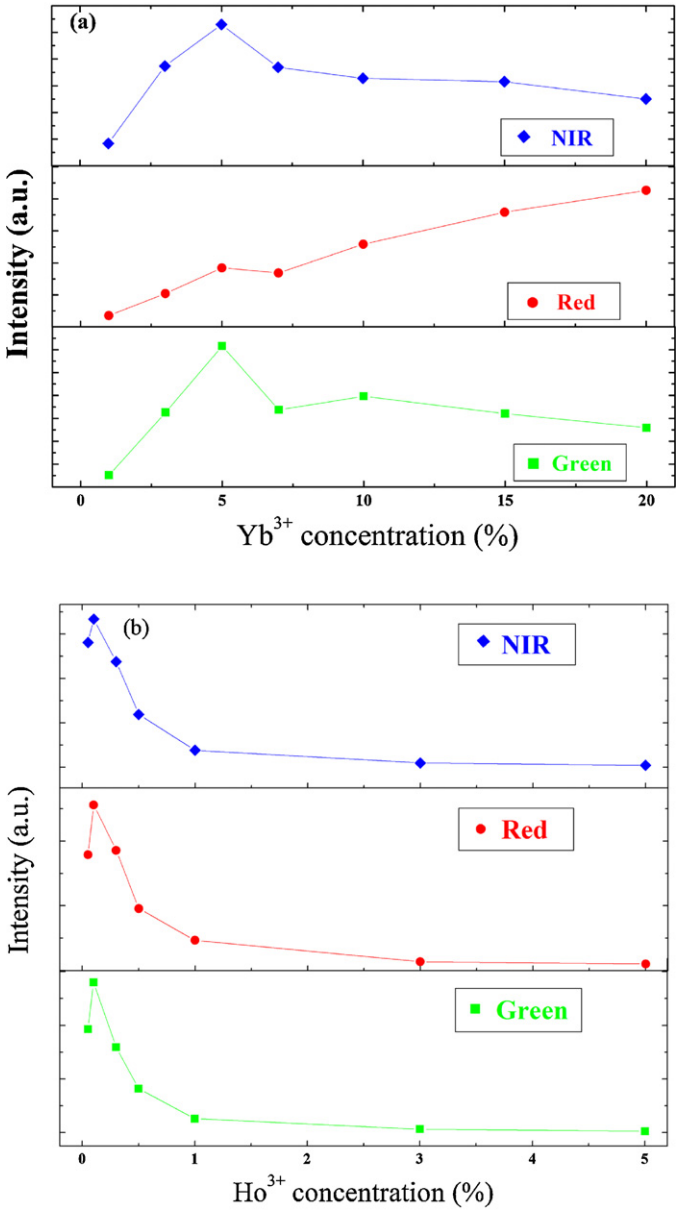

Fig. 5. Dependences of UC emission intensities on Yb^{3+} (a) and Ho^{3+} (b) concentrations.

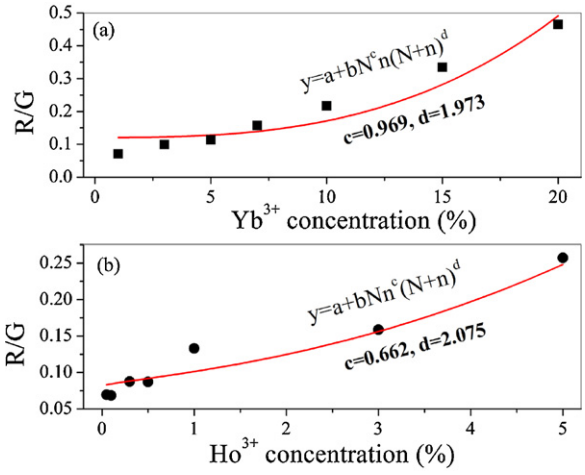

Fig. 6. Dependences of the ratio of the red UC emission intensity to that of the green one on Yb^{3+} (a) and Ho^{3+} (b) concentrations.

its population, as depicted in Fig. 4. In Fig. 5(b), it can be found that with the increase of Ho^{3+} concentration, all UC emission intensities increase first and then decrease due to the concentration quenching effect. And when Yb^{3+} concentration is 5%, the optimum Ho^{3+} concentration is about 0.1%.

Fig. 6 shows the dependences of the UC emission intensity ratio of red to green (R/G) on Yb^{3+} and Ho^{3+} concentrations. As can be seen, the R/G ratio increases with both Yb^{3+} and Ho^{3+} concentrations in our experimental concentration range, which further confirm that Ho^{3+} $^5F_5$ level has different populated way.

To comprehensively understand the UC process of Ho^{3+}/Yb^{3+} co-doped system, a set of rate equations was established based upon the energy levels diagram (as shown in Fig. 4) and the above UC mechanism analysis, and is given below [28]:

$$\frac{dn_1}{dt} = n_5W_{51} + n_4W_{41} + n_3W_{31} + n_2W_{21} - C_{b3}n_1N_b \tag{3}$$

$$\frac{dn_2}{dt} = (W_{n32} + W_{32})n_3 - n_2W_{21} - C_{b4}n_2N_b + n_5W_{52} - C_{43}n_2n_5 \tag{4}$$

$$\frac{dn_3}{dt} = C_{b3}n_1N_b - C_{b5}n_3N_b - n_3W_{31} - (W_{n32} + W_{32})n_3 + C_{43}n_2n_5 \tag{5}$$

$$\frac{dn_4}{dt} = C_{b4}n_2N_b - n_4W_{41} + C_{43}n_2n_5 \tag{6}$$

$$\frac{dn_5}{dt} = C_{b5}n_3N_b - (W_{51} + W_{52})n_5 - C_{43}n_2n_5 \tag{7}$$

$$\frac{dN_b}{dt} = R_{ab}\Phi N_a - A_{ba}N_b - C_{b3}n_1N_b - C_{b4}n_2N_b - C_{b5}n_3N_b \tag{8}$$

$$\frac{dN_a}{dt} = -R_{ab}\phi N_a + A_{ba}N_b + C_{b3}n_1N_b + C_{b4}n_2N_b + C_{b5}n_3N_b \tag{9}$$

$$N_a + N_b = N \tag{10}$$

$$n_1 + n_2 + n_3 + n_4 + n_5 = n \tag{11}$$

where N_a and N_b represent the population densities of Yb^{3+} in ground and excited states, n_i represent the population density of the ith level of Ho^{3+} marked in Fig. 4, where $i \in \{1, 2, 3, 4, 5\}$. N and n are the total concentrations of Yb^{3+} and Ho^{3+} ions, A_{ba} and R_{ab} are the radiation and absorption transition rates of Yb^{3+}, Φ is the incident pumping flux, W_{ij} and W_{nij} are the radiative and non-radiative transition rates of Ho^{3+}, C_{ij} and C_{bi} are the net cross relaxation and ET rates.

In the case of continuous wave laser excitation, the left terms in Eqs. (3)–(9) would be equal to zero. From Figs. 2 and 3, it was observed that the red emission ($^5F_5 \rightarrow {}^5I_8$) is much weaker than the green one ($^5S_2$, $^5F_4 \rightarrow {}^5I_8$) at low Yb^{3+}-concentration doping case, thus the depopulation of ($^5S_2$, $^5F_4$) levels by ET ($^5S_2$, $^5F_4$) + $^5I_7 \rightarrow {}^5F_5 + {}^5I_6$ can be neglected. Therefore, it can be readily gotten

$$n_5 = \frac{C_{b5}N_bn_3}{W_{51} + W_{52}}. \tag{12}$$

Similarly,

$$n_3 = \frac{C_{b3}N_bn_1}{W_{31} + W_{n32} + W_{32} + C_{b5}N_b}. \tag{13}$$

Through Eqs. (12) and (13), n_5 can be expressed as

$$n_5 = \frac{C_{b3}C_{b5}N_b^2n_1}{(W_{51} + W_{52})(W_{31} + W_{32} + W_{n32} + C_{b5}N_b)}. \tag{14}$$

From Eq. (6), n_4 can be expressed as

$$n_4 = \frac{C_{b4}n_2N_b + C_{43}n_2n_5}{W_{41}}. \tag{15}$$

Considering the weak NIR UC emission, $^5I_7$ level cannot be populated effectively by radiative transition from ($^5S_2$, $^5F_4$) levels, so the population of $^5I_7$ level can be mainly ascribed to the radiative transition and nonradiative relaxation from $^5I_6$ level. $^5I_7$ level is mainly depopulated via radiative transition and ET processes, and finally gets into $^5I_8$ level or $^5F_5$ level. However, the ET process can be neglected since the red UC emission is weak. Therefore, the terms $C_{43}n_2n_5$, n_5W_{52} and $C_{b4}n_2N_b$ can be neglected, n_2 would be then written as

$$n_2 = \frac{(W_{32} + W_{n32})n_3}{W_{21}} \tag{16}$$

Combining Eqs. (13), (14), (15) and (16), n_4 can be written as

$$n_4 = \frac{C_{b3}C_{b4}N_b^2n_1(W_{32} + W_{n32})}{W_{21}(W_{31} + W_{n32} + W_{32} + C_{b5}N_b)W_{41}} + \frac{C_{43}C_{b3}^2C_{b5}N_b^3n_1^2(W_{n32} + W_{32})}{W_{21}(W_{31} + W_{n32} + W_{32} + C_{b5}N_b)^2W_{41}(W_{51} + W_{52})} \tag{17}$$

Considering the low excitation density case, the ET rate from Yb^{3+} to Ho^{3+} could be smaller than the radiative transition rate from $^2F_{5/2} \rightarrow {}^2F_{7/2}$ of Yb^{3+}. Thus, from Eq. (8), N_b can be

expressed as

$$N_b = \frac{R_{ab}\Phi N_a}{A_{ba}} \tag{18}$$

Besides, in the case of low density excitation, the ground states of Ho^{3+} and Yb^{3+} cannot be effectively depopulated. Thus, n_1 and N_a are equal to the total concentrations of n (Ho^{3+}) and N (Yb^{3+}), respectively. The ratio n_4/n_5 can be obtained as:

$$n_4/n_5 = \frac{C_{b4}(W_{51}+W_{52})(W_{n32}+W_{32})}{C_{b5}W_{21}W_{41}} + \frac{(W_{n32}+W_{32})C_{43}C_{b3}N\Phi R_{ab}n}{A_{ba}W_{41}W_{21}(W_{31}+W_{32}+W_{n32}+C_{b5}N_b)}. \tag{19}$$

Generally, the dipole–dipole interaction between luminescent centers is the most effective pathway of ET and its rate satisfies the following form [29]:

$$P_{ET} = f\left(\frac{R_0}{R}\right)^6 \tag{20}$$

where f is a phenomenological parameter, R is the distance between the nearest ions, and R_0 is the critical transfer distance where the ET rate is equal to the spontaneous emission rate. Considering $1/(N+n) \propto 4\pi R^3/3$, the ET rates C_{bi} can be expressed as follows:

$$C_{bi} = f_i\left(\frac{R_{0i}}{R}\right)^6, \quad i \in \{3,4,5\} \tag{21}$$

where f_i and R_{0i} are the phenomenological parameter and the critical transfer distance of each ET process. At last, the ET rates C_{bi} can be formally written as

$$C_{bi} = C_i(N+n)^2, \quad i \in \{3,4,5\} \tag{22}$$

where $C_i = f_i(R_{0i})^6$. The ratio n_4/n_5 can be expressed as:

$$n_4/n_5 = \frac{C_4(W_{51}+W_{52})(W_{n32}+W_{32})}{C_5W_{21}W_{41}} + \frac{(W_{n32}+W_{32})C_{43}C_{b3}Nn(N+n)^2\Phi R_{ab}}{A_{ba}W_{41}W_{21}(W_{31}+W_{32}+W_{n32}+C_{b5}N_b)} \tag{23}$$

Then, Eq. (23) can be simplified as

$$n_4/n_5 = a + bNn(N+n)^2 \tag{24}$$

where

$$a = \frac{C_4(W_{51}+W_{52})(W_{n32}+W_{32})}{C_5W_{21}W_{41}}$$

and

$$b = \frac{(W_{n32}+W_{32})C_{43}C_{b3}\Phi R_{ab}}{A_{ba}W_{41}W_{21}(W_{31}+W_{32}+W_{n32}+C_{b5}N_b)}$$

Eq. (24) describes the relationship between the ratio of population density and the doping concentrations of Ho^{3+} and Yb^{3+}, which reflects the dependence of R/G on Ho^{3+} and Yb^{3+} doping concentrations since the emissions are proportional to the population of emitting levels. Thus, we take Eq. (24) as the theoretical formula to fit the experimental data in Fig. 6. It can be found that the experimental data can be fitted well with Eq. (24). The parameters c and d are 0.969, 1.973 for Yb^{3+}-concentration varied case and 0.662, 2.075 for Ho^{3+}-concentration varied case, respectively. The obtained free parameter c and d values are very close to the theoretical values in the Eq. (24), indicating Eq. (24) may be a suitable theoretical formula for describing the relationship of UC emission intensity with Yb^{3+} and Ho^{3+} concentrations in our studied system. Meanwhile, the result could explain the different trends between the red emission and the green one as Yb^{3+} and Ho^{3+} concentrations increase.

3.4. UC luminescence properties evaluation

In order to evaluate the UC luminescence properties of our prepared samples, commercial Er^{3+}/Yb^{3+} co-doped $NaYF_4$ material was used as a reference, which has been recognized as one of the most efficient UC luminescence material [30]. Fig. 7 shows the intensity ratio of the optimized concentration sample with 0.1% Ho^{3+}/5% Yb^{3+} and $NaYF_4$:Er^{3+}/Yb^{3+} under the same measured condition with LD working current range from 0.3 A to 1.6 A. It can be found that the ratio increases dramatically with the increase of LD working current and the sample we prepared has a comparable intensity with $NaYF_4$:Er^{3+}/Yb^{3+} at higher working current. Besides, as can be seen from Fig. 3(b), the optimized sample we prepared has a strong green emission accompanied with very weak red and NIR emissions, showing a good color performance. However, the UC spectrum of $NaYF_4$:Er^{3+}/Yb^{3+} exhibits two dominant emission peaks corresponding to green and red emissions as shown in the inset of Fig. 7, showing a slightly worse color performance. In addition, compared with fluoride $NaYF_4$, $NaGdTiO_4$ as an oxide is more easily prepared and has better chemical and thermal stability. Therefore, $NaGdTiO_4$:Ho^{3+}/Yb^{3+} may be a good green UC luminescence material and has potential applications in high temperature and hash environments.

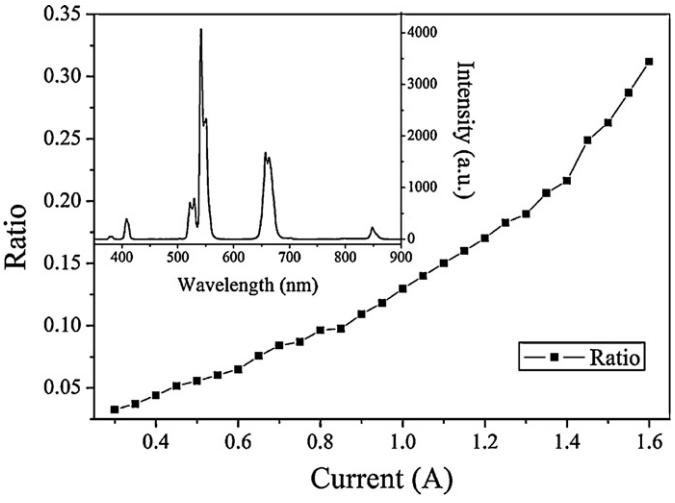

Fig. 7. Dependences of UC emission intensity ratio of $NaGdTiO_4$:Ho^{3+}/Yb^{3+} to commercial $NaYF_4$:Er^{3+}/Yb^{3+} on LD working current. The inset is the UC emission spectrum of $NaYF_4$:Er^{3+}/Yb^{3+} excited by 980 nm LD.

4. Conclusions

Ho^{3+}/Yb^{3+} co-doped $NaGdTiO_4$ phosphors with various concentrations were synthesized via a conventional solid-state reaction method. The dependence of UC luminescence on excitation power density was studied. It was found that two-photon processes are responsible for all of green, red and NIR UC emissions in various Ho^{3+} and Yb^{3+} concentrations doping cases. The concentration dependences of green, red and NIR UC luminescence studies showed that the UC luminescence intensities changed strongly with Ho^{3+} concentration but weakly with Yb^{3+} concentration. The UC emission intensity ratio of $^5I_5 \rightarrow {}^5I_8$ to $(^5S_2, {}^5F_4) \rightarrow {}^5I_8$ transitions was also dependent on Yb^{3+} and Ho^{3+} concentrations. In order to better understand this process, rate equations were established based on the possible UC mechanisms and a theoretical formula was proposed to describe the concentration dependent UC emission. Finally, the UC luminescence properties of the presented material were estimated and the results showed that the sample presented here possessed very high UC luminescence efficiency and good color performance.

Acknowledgments

This work was supported by the NSFC (National Natural Science Foundation of China, Grant Nos. 50972021, 11104023, 61078061 and 11104024), the China Postdoctoral Science Foundation (Grant No. 20110491539), the Scientific Research Foundation for Doctoral Program of Liaoning Province of China (Grant Nos. 20111032 and 20111031), and the Fundamental Research Funds for the Central Universities (Grant Nos. 2011JC36, 2011ZD032, 2011ZD033, 2011QN152 and 2011JC37).

References

[1] J. Méndez-Ramos, V.K. Tikhomirov, V.D. Rodríguez, D. Furniss, Infrared tuneable up-conversion phosphor based on Er^{3+}-doped nano-glass–ceramics, J. Alloys Compd. 440 (2007) 328–334.

[2] X.B. Chen, Z.F. Song, N. Sawanobori, M. Ohtsuka, X.W. Li, Y.F. Wang, X.L. Xu, C.J. He, H. Ma, Y. Chen, J.Y. Zhu, The characteristic saturation phenomenon of upconversion luminescence in holmium–ytterbium-co-doped oxyfluoride glass Ho(0.1)Yb(5):FOG, Physica B 403 (2008) 3847–3852.

[3] M. Ma, C.F. Xu, L.W. Yang, G.Z. Ren, J.G. Lin, Q.B. Yang, Intense ultraviolet and blue upconversion emissions in Yb^{3+}–Tm^{3+} codoped stoichiometric $Y_7O_6F_9$ powder, Physica B 406 (2011) 3256–3260.

[4] Y. Kishi, S. Tanabe, S. Tochino, G. Pezzotti, Fabrication and efficient infrared-to-visible upconversion in transparent glass ceramics of Er–Yb co-doped CaF_2 nano-crystals, J. Am. Ceram. Soc. 88 (2005) 3423–3426.

[5] H.T. Sun, S.X. Dai, S.Q. Xu, J.J. Zhang, L.L. Hu, Z.H. Jiang, Efficient frequency upconversion emission of Er^{3+}/Yb^{3+}-codoped potassium–magnesium–lead–bismuth glasses pumped at 975 nm, Physica B 352 (2004) 366–371.

[6] X.X. Zhang, P. Hong, M. Bass, B.H.T. Chai, Ho^{3+} to Yb^{3+} back transfer and thermal quenching of upconversion green emission in fluoride crystals, Appl. Phys. Lett. 63 (1993) 2606–2608.

[7] J. Li, J.Y. Wang, H. Tan, X.F. Cheng, F. Song, H.J. Zhang, S.R. Zhao, Growth and thermal properties of $Sm:YAl_3(BO_3)_4$ crystal, J. Cryst. Growth 256 (2003) 324–327.

[8] A.V. Kiryanov, V. Aboites, A.M. Belovolov, M.J. Damzen, A. Minassian, M.I. Timoshechkin, M.I. Belovolov, Visible-to-near-IR luminescence at stepwise up-conversion in Yb, Ho:GGG under IR diode pumping, J. Lumin. 102–103 (2003) 715–721.

[9] I.R. Marin, V.D. Rodríguez, V. Lavín, U.R. Rodríguez-Mendoza, Upconversion dynamics in Yb^{3+}–Ho^{3+} doped fluoroindate glasses, J. Alloys Compd. 275–277 (1998) 345–348.

[10] L.F. Johnson, H.J. Guggenheim, Infrared-pumped visible laser, Appl. Phys. Lett. 19 (1971) 44–47.

[11] E. De la Rosa, P. Salas, H. Desirena, C. Angeles, R.A. Rodriguez, Strong green upconversion emission in $ZrO_2:Yb^{3+}$–Ho^{3+} nanocrystals, Appl. Phys. Lett. 87 (2005) 241912.

[12] F. Lahoz, R. Martin, A. Briones, Infrared-laser induced photon avalanche upconversion in Ho^{3+}–Yb^{3+} codoped fluoroindate glasses, J. Appl. Phys. 95 (2004) 2957–2962.

[13] Y. Wang, W.P. Qin, J.S. Zhang, C.Y. Cao, J.S. Zhang, Y. Jin, Synthesis of colloidal LaF_3:0.04Yb^{3+}, 0.01Er^{3+} nanocrystals with green upconversion luminescence, J. Rare Earth 26 (2008) 40–43.

[14] W. Lozano B, B. Cid, de Araújo, L.H. Acioli, Y. Messaddeq, Negative nonlinear absorption in Er^{3+}-doped fluoroindate glass, J. Appl. Phys. 84 (1998) 2263–2267.

[15] X.P. Chen, W.J. Zhang, Q.Y. Zhang, Towards efficient upconversion and downconversion of $NaYF_4:Ho^{3+},Yb^{3+}$ phosphors, Physica B 406 (2011) 1248–1252.

[16] T. Hirai, T. Orikoshi, Preparation of Gd_2O_3:Yb, Er and Gd_2O_2S:Yb, Er infrared to visible conversion phosphor fine ultrafine particles using an emulsion liquid membrane system, J. Colloid Interface Sci. 273 (2004) 470–477.

[17] X.X. Luo, W.H. Cao, Upconversion luminescence of holmium and ytterbium co-doped yttrium oxysulfide phosphor, Mater. Lett. 61 (2007) 3696–3700.

[18] J.C. Boyer, F. Vertrone, J.A. Capobianco, A. Speghini, M. Zambelli, M. Bettinelli, Investigation of the upconversion processes in nanocrystalline $Gd_3Ga_5O_{12}:Ho^{3+}$, J. Lumin. 106 (2004) 263–268.

[19] L.Q. An, J. Zhang, M. Liu, S.W. Wang, Preparation and upconversion properties of Yb^{3+}, Ho^{3+}:Lu_2O_3 nanocrystalline powders, J. Am. Ceram. Soc. 88 (2005) 1010–1012.

[20] W.L. Lu, L.H. Cheng, J.S. Sun, H.Y. Zhong, X.P. Li, Y. Tian, J. Wan, Y.F. Zheng, L.B. Huang, T.T. Yu, H.Q. Yu, B.J. Chen, The concentration effect of upconversion luminescence properties in Er^{3+}/Yb^{3+}-codoped $Y_2(MoO_4)_3$ phosphors, Physica B 405 (2010) 3284–3288.

[21] T. Hirai, T. Orikoshi, I. Komasawa, Preparation of Y_2O_3:Yb, Er Infrared-to-visible conversion phosphor fine particles using an emulsion liquid membrane system, Chem. Mater. 14 (2002) 3576–3583.

[22] L. Li, X.C. Wang, X.T. Wei, Y.H. Chen, C.X. Guo, M. Yin, Influence of precipitant solution pH on the structural, morphological and upconversion luminescent properties of Lu_2O_3:2%Yb, 0.2%Tm nanopowders, Physica B 406 (2011) 609–613.

[23] W.L. Lu, L.H. Cheng, H.Y. Zhong, J.S. Sun, J. Wan, Y. Tian, B.J. Chen, Dependence of upconversion emission intensity on Yb^{3+} concentration in Er^{3+}/Yb^{3+} co-doped flake shaped $Y_2(MoO_4)_3$ phosphors, J. Phys. D: Appl. Phys. 43 (2010) 085404.

[24] J.C. Boyer, F. Vetrone, J.A. Capobianco, A. Speghini, M. Bettinelli, Yb^{3+} ion as a sensitizer for the upconversion luminescence in nanocrystalline $Gd_3Ga_5O_{12}:Ho^{3+}$, Chem. Phys. Lett. 390 (2004) 403–407.

[25] G.D. Gilliland, R.C. Powell, L. Esterowitz, Spectral and up-conversion dynamics and their relationship to the laser properties of $BaYb_2F_8:Ho^{3+}$, Phys. Rev. B 38 (1988) 9958–9973.

[26] S. Xiao, X. Yang, Z. Liu, X.H. Yan, Up-conversion in Er^{3+}:Y_2O_3 nanocrystals pumped at 808 nm, J. Appl. Phys. 96 (2004) 1360–1364.

[27] A. Diening, S. Kück, Spectroscopy and diode-pumped laser oscillation of Yb^{3+}, Ho^{3+}-doped yttrium scandium gallium garnet, J. Appl. Phys. 87 (2000) 4063–4068.

[28] X.L. Yang, S.G. Xiao, Z.W. Liu, X.H. Yan, Sensitizer-dependent upconversion of Ho^{3+} in nanocrystalline Y_2O_3, Appl. Phys. B 86 (2007) 77–82.

[29] F. Auzel, Upconversion and anti-Stokes processes with f and d ions in solids, Chem. Rev. 104 (2004) 139–173.

[30] K.W. Kramer, D. Biner, G. Frei, H.U. Gudel, M.P. Hehlen, S.R. Luthi, Hexagonal sodium yttrium fluoride based green and blue emitting upconversion phosphors, Chem. Mater. 16 (2004) 1244–1251.